Carbohydrate Polymers 90 (2012) 1265–1272

Contents lists available at SciVerse ScienceDirect

Carbohydrate Polymers

journal homepage: www.elsevier.com/locate/carbpol

Synthesis of chitosan networks: Swelling, drug release, and magnetically assisted BSA separation using Fe_3O_4 nanoparticles

Mousa Ghaemy*, Motahare Naseri

Polymer Research Laboratory, Department of Chemistry, University of Mazandaran, Babolsar, 47416-95447, Iran

ARTICLE INFO

Article history:
Received 5 May 2012
Received in revised form 12 June 2012
Accepted 23 June 2012
Available online 2 July 2012

Keywords:
Chitosan
Nanohydrogel
Swelling
SDF loading and releasing
Fe_3O_4 nanoparticles
BSA protein

ABSTRACT

Chitosan (CS) nanohydrogel networks were prepared by reaction with glyceroldiglycidylether (GDE) and poly(dimethylsiloxane) (PDMS), as crosslinking agents in an emulsion system. The nanogel content increased with increasing the amount of crosslinkers and reached to a maximum of 90% with GDE. The nanogels structure was characterized by FT-IR, AFM, DSC, and TGA. The average size for CS-GDE and CS-PDMS particles were 59 nm and 180 nm, respectively. The swelling behavior of nanohydrogels was observed to be dependent on pH, temperature, degree of crosslinking, and on the chemical structure of crosslinker. The equilibrium water content of CS-GDE nanohydrogels reached to a maximum of 600% at neutral pH, and decreased at high and low pH and low temperature. These nanohydrogels were tested for sodium diclofenac (SDF) loading and releasing efficiency. The covalent conjugation of bovine serum albumin (BSA) and magnetic Fe_3O_4 nanoparticles on the hydrogels were found to hold a potential application in magnetically assisted bioseparation.

1. Introduction

Chitosan is currently receiving enormous interest for medical and pharmaceutical applications due to its biocompatibility in animal tissues, biodegradability (Borzacchiello et al., 2001; Kumar, Muzzarelli, Muzzarelli, Sashiwa, & Domb, 2004; Muzzarelli, 2011; Muzzarelli, Boudrant, et al., 2012; Muzzarelli, Greco, Busilacchi, & Gigante, 2012; Senel & McClure, 2004) and its degradation products are nontoxic, non-immunogenic and non-carcinogenic (Felt, Buri, & Gurny, 1998; Muzzarelli, 2010). Chitosan based hydrogels have good biocompatibility, low degradation and processing ease yielding well-defined physicochemical properties and easily reproducible drug release profiles (Chen & Hoffman, 1995; Muzzarelli, 2009; Sokker, Abdel Ghaffar, Gad, & Aly, 2009; Tao, Pang, Chen, Ren, & Hu, 2012). Considerable efforts are especially directed at modifying CS to improve its solubility in water (Hirano, Yamaguchi, & Kamiya, 2003; Sashiwa, Yamamori, Ichinose, Sunamoto, & Aiba, 2003; Verma, Deshpande, & Kennedy, 2004; Zhou, Yang, Wang, & Liu, 2003). Cross-linked hydrogels are three-dimensional macromolecular networks, hydrophilic, capable to absorb large amounts of water or biological fluids. One of the most convenient and effective approaches to modify the properties of chitosan hydrogels consists in its crosslinking. The hydroxyl and amino groups on glucosamine units of chitosan provide the reactive sites for crosslinking reactions (Bajpai & Rasika, 2006; Enescu et al., 2009; Yanga et al., 2010; Yu, Hu, Pan, Yao, & Jiang, 2006).

Magnetic separation is a recent developing technology that is mostly applied in the field of bioseparation. Many previous works have been focused on the application of the magnetic separation of the enzyme immobilization (Kato, Onishi, & Machida, 2003), cell sorting (George & Abraham, 2006; Prabaharan & Mano, 2006; Sharma, Kulkarni, & Pawar, 2006), protein adsorption and purification (Bernkop-Schnurch & Walker, 2001; van der Lubben, Verhoef, Borchard, & Junginger, 2001), nucleic acid detachment (Fan, Wang, Fan, & Ma, 2006; Shutava & Lvov, 2006), and drug delivery (Pandey, Ahmad, Sharma, & Khuller, 2005).The greatest advantage of super paramagnetic nanoparticles is related to their fast and facile separation by implementing an external magnetic field (Ah, Salabas, & Schuth, 2007). Covalent conjugated proteins on nanoparticles have wide applications in drug targeting and are highly sensitive immunoassay. A simple method was proposed (Mehta, Upadhyay, Charles, & Ramchand, 1997) to bind the protein covalently on the magnetic nanoparticles via carbodiimide activation. In that study they found that BSA could be covalently bound to magnetic particles while maintaining its biological properties. Recently, carbodiimide was also used to activate the direct adsorption of protein on magnetic particles (Yu et al., 2009). So far separation of BSA using magnetic Fe_3O_4 nanoparticles covalently bounded on the chitosan nanohydrogel networks have not been investigated.

In the present study chitosan nanohydrogel networks are synthesized with GDE and PDMS as crosslinkers in an emulsion media.

* Corresponding author. Tel.: +98 112 534 2353; fax: +98 112 534 2302.
E-mail address: ghaemy@umz.ac.ir (M. Ghaemy).

0144-8617/$ – see front matter © 2012 Elsevier Ltd. All rights reserved.
http://dx.doi.org/10.1016/j.carbpol.2012.06.069

The structure of nanohydrogels is investigated by FT-IR, AFM, gel percent, water swelling behavior, and thermal properties. Loading and release efficiency of SDF drug in the nanohydrogel networks are studied. We also report a single-step solution-based method of covalently binding of BSA protein on the magnetic Fe_3O_4 nanoparticles during formation of chitosan hydrogel network. Separation efficiency of BSA from neat and magnetite chitosan hydrogel network is compared by using conventional separation method and an external magnetic field.

2. Experimental

2.1. Materials and instrumentals

Chitosan of molecular weight in the range of 10^5–3×10^5 g/mol and degree of deacetylation ≥75% (9012-76-4), Span 40 (non-ionic surfactant; 26266-57-9), glacial acetic acid (100%), both ends epoxy terminated crosslinkers of glycerol diglycidyl ether (GDE, 204 g/mol; 27043-36-3) and poly(dimethylsiloxane) (PDMS, 800 g/mol; 130167-23-6) were from Fluka Co. (Germany). Sodium diclofenac (SDF) was from a pharmaceutical industry in Iran (Jaberebne Hayan Pharmaceutical Co.). Iron (II) chloride tetrahydrate ($FeCl_2{\cdot}4H_2O$, 98%) and iron (III) chloride hexahydrate ($FeCl_3{\cdot}6H_2O$, 99%) were from Applichem and Scharlau companies, respectively. Carbodiimide (1-ethyl-3(3-dimethylaminopropyl), EDC; 1892-57-5) was from Sigma–Aldrich chemical Co. and BSA from Merck biochemical Co. (9048-46-8).

FT-IR spectra were recorded on a spectrophotometer of Bruker Tensor 27 (Germany). About 2 mg of the sample were grounded thoroughly with KBr and pellets were prepared using hydraulic press under a pressure of 600 kg/cm^2. Shimadzu UV spectrophotometer was used for reading maximum absorption of SDF. Differential scanning calorimetry (DSC) and thermo gravimetric analysis (TGA) were recorded on a Stanton Redcraft STA-780 (London, UK). DSC and TGA curves were recorded at 10 °C/min under N_2 from ambient temperature up to 300 °C and 600 °C, respectively. AFM, Easy Scan 2 Flex AFM (Swiss Co), and SEM, Seron Technology AIS 2100, was used to investigate the surface property of nanohydrogels. An electromagnet magnetic separator (NB22A, Electroprístroj, Czech Republic) was used for the separation of BSA protein from hydrogel. PH meter Metrohm 827, accuracy ± 0.1 (Switzerland). Centrifuge, Hettich Rotanta model MIKRO 22R (Kirchlengern, Germany).

2.2. Synthesis of crosslinked chitosan nanohydrogels

Firstly, a solution was prepared by dissolving 0.50 g chitosan powder in 50 mL acetic acid aqueous solution (4%). The mixture was stirred for 20 min at room temperature to obtain a homogeneous viscous solution. Span 40, a non-ionic, surfactant (0.0054 g) was added to the mixture and after 1 h stirring (at 1000 rpm, at 60 °C) with a mechanical stirrer, different amounts of crosslinking agent of GDE and PDMS (from 5 to 40 wt%) were added to the dispersion medium and stirring was continued for a further 12 h. The solutions were then neutralized with 0.5 M NaOH solution and checked by using a pH meter, and then centrifuged for 20 min at 80 rev min^{-1} to separate the solid product which was dried in a vacuum oven at 40 °C. The neutralized crosslinked nanohydrogels were hot extracted in a Soxhlet with 1% aqueous acetic acid solution for 12 h to remove uncrosslinked chitosan. The crosslinked chitosan was washed several times with distilled water followed by acetone to remove unreacted crosslinker. The samples were dried at 40 °C in a vacuum oven for 24 h. The percent of insoluble part or percent of gel (Gel, %), which indicates the amount of crosslinked chitosan was calculated from the increase in weight of chitosan after crosslinking reaction as follows (Bajpai & Rasika, 2006).

$$\text{Gel}\,(\%) = \frac{W_d}{W_i} \times 100$$

where W_d is the weight of dry gel after extraction and W_i is the initial weight of dry gel.

2.3. Water swelling behavior

Swelling behavior of the crosslinked chitosan nanohydrogels was determined by equilibrium swelling studies, according to a recently published procedure (Yanga et al., 2010). The dried samples were cut into small pieces of 1 cm × 1 cm, precisely weighed and submerged into deionized water for different periods of time at room temperature until equilibrium was reached. At each immersion interval, the swollen samples were removed from water, wiped off excess water on surface with filter tissue paper and immediately weighed. The initial sample weight before immersion was recorded as W_d and the sample weight after each immersion interval was recorded as W_s. The swelling percent at equilibrium, WS%, was calculated from the following equation:

$$\text{WS\%} = \frac{W_s - W_d}{W_d} \times 100$$

The effect of pH and temperature of the swelling media on the swelling behavior of nanohydrogels was also investigated. Buffer solutions of pH = 3, 5, 7 and 9 were used to study the pH-sensitivity of nanohydrogels for a period of 60 min. The pH values were precisely checked by a pH meter (Metrohm 827, accuracy ± 0.1). Three different temperatures of 60 °C, 40 °C and room temperature (~25 °C) were used to study the swelling behavior of the nanohydrogels.

2.4. Drug loading and releasing procedure

SDF was used as a model drug for loading and release experiment. 1 g of a nanohydrogel network was added to a 100 mL stoppered glass bottle containing 50 mL aqueous solution of different percents of SDF (0.25, 0.5, 0.75, or 1%, w/v) at pH = 7.4. The bottles were shaken at 150 rpm for 24 h. Then the content of the bottle was filtered and the maximum wavelength of absorption of SDF in the filtrate was determined at 276 nm. The concentration of SDF in the filtrate was determined by using the absorption wavelength and a calibration curve, which was made for different concentrations of SDF in distilled water. The amount of SDF entrapped in the matrices was calculated from the difference between the total amount of SDF added and the SDF found in the filtrate. The swollen nanohydrogels loaded with SDF were dried in a vacuum oven at 37 °C. To study the release profiles of drug-loaded nanohydrogels, the previously dried SDF loaded samples were immersed into 100 mL of a buffer solution of pH = 7.4 at 37 °C. At specific time intervals 3 mL of solution was withdrawn, and the released SDF percent was calculated by using maximum wavelength of absorption at 276 nm and the calibration curve.

2.5. Preparation of super paramagnetic Fe_3O_4 nanoparticles

Nanosized magnetic particles (Fe_3O_4) were prepared by using the chemical precipitation method using Fe^{2+}, Fe^{3+} salts, and ammonium hydroxide under a nitrogen atmosphere (Peng, Hidajat, & Uddin, 2004). A mixture of 0.01 M $FeCl_3{\cdot}6H_2O$ (50 mL) and 0.005 M $FeCl_2{\cdot}4H_2O$ (50 mL) was stirred on a magnetic stirrer plate. Then, 2 mL of NH_4OH solution (25%) was added rapidly into the solution with vigorous stirring, and it continued until the pH value

of the solution reached 10. Afterward, the solution was stirred for additional 45 min. Finally, the Fe_3O_4 nanoparticles were collected by magnetic field separation, washed with and then dispersed in distilled water. Therefore, the covalent conjugation of protein onto the magnetic nanoparticles could be carried out in aqueous solution.

2.6. Covalent conjugation of BSA protein and magnetic Fe_3O_4 nanoparticles into hydrogel

Adsorption of bovine serum albumin (BSA) on nanosized magnetic particles (Fe_3O_4) was carried out in the presence of carbodiimide (Peng et al., 2004; Wang & Lee, 2003). Covalent binding of BSA protein and magnetic Fe_3O_4 nanoparticles into chitosan hydrogel network was carried out simultaneously in a three necked round-bottomed flask equipped with three dropping funnels. 0.5 g CS was dissolved in 4% (v/v) acetic acid solution. 1 mL magnetic Fe_3O_4 nanoparticles solution (8.9 g/L, i.e., 38.4 mM), 150 μL BSA protein solution (1 g/L BSA) containing a small aliquot of carbodiimide solution (57 mM), and 12 mL GDE crosslinker was placed separately in each dropping funnel. These solutions were added dropwise to the chitosan solution simultaneously and the whole mixture was stirred at room temperature for 72 h. Then water was evaporated from the suspension solution and the crosslinked hydrogels with embedded BSA and magnetic Fe_3O_4 nanoparticles were obtained.

2.7. Separation of magnetic affinity biopolymer adsorbent

After immobilization of the BSA protein and Fe_3O_4 nanoparticles into the chitosan hydrogel network, an appropriate amount of mixture with total volume of about 1 L was placed in the flat flask situated in vertical position and was exposed to a magnetic field provided by an electromagnet magnetic separator, power supply could be set to the voltage up to 30 V. The particles with high magnetic sensitivity attached to the wall of the separator flask for duration of 10–20 min, while low magnetic or nonmagnetic particles accumulated at the bottom of the flask or remained in the suspension and were removed. Magnetic susceptibility was measured using the magnetic sensor of 4 ampere (MS2B Bartington Instruments, UK). At each step of the separation, the magnetic separator collected part of the nanoparticles and analyzed them for the BSA content, indicating the amount of BSA, bounded on the nanoparticles. To collect most of the nanoparticles efficiently, the separator was required to be operated for multiple separation steps.

3. Results and discussion

3.1. Preparation of nanohydrogel networks

Chitosan nanohydrogel network was prepared by simultaneous grafting and crosslinking reactions with PDMS and GDE crosslinkers. It is well known that the primary amine quickly undergo nucleophilic substitution reaction with the epoxide ring and form secondary amino group which undergo a second substitution reaction yielding tertiary amine. These reactions between amine groups of chitosan and epoxide rings were carried out in an emulsion system with mechanical stirring at 1000 rpm (at 60 °C). Although the solubility parameters of chitosan and PDMS containing siloxane or silane moieties are different but the emulsion conditions was used to enhance the miscibility between these starting materials. Also, PDMS with both ends epoxide rings in reaction with amine form diols at each PDMS terminal. The amphiphilic characteristics due to the formation of hydrophilic hydroxyl terminals apparently enhanced the miscibility between PDMS and chitosan. This phenomenon was evidenced by the significantly high concentration of PDMS that was introduced into chitosan structure. It is hypothesized that the hydroxyl terminals formed hydrogen bonding with chitosan and left PDMS backbone to aggregate microscopically inside the networks.

Table 1
Weight percent of the crosslinked nanohydrogels.

wt% cross-linker	Code	Gel fraction (%)
5% GDE	CS-GDE5	70.00
10% GDE	CS-GDE10	76.00
20% GDE	CS-GDE20	85.00
30% GDE	CS-GDE30	91.00
40% GDE	CS-GDE40	89.00
5% PDMS	CS-PDMS5	67.00
10% PDMS	CS-PDMS10	73.00
20% PDMS	CS-PDMS20	81.00
30% PDMS	CS-PDMS30	79.00

CS = chitosan, GDE = glycerol diglycidyl ether, PDMS = poly(dimethylsiloxane).

FT-IR spectrum of neat chitosan shows the strong basic characteristics peak at 3423 cm^{-1} related to the axial stretching vibration of O—H superposed to the N—H stretching band. Also there are characteristics peaks at 2924 cm^{-1} of C—H stretching of methyl or methylene group, at 1578 cm^{-1} of N—H bending, at 1656 cm^{-1} due to carbonyl stretching vibration of the remained acetamide group and a broad band appearing around 1115 cm^{-1} indicates the C—O stretching vibration. Following the chemical modification of chitosan, the absorption band at 1578 cm^{-1} is moved to 1560 cm^{-1}, and peaks at 1115 cm^{-1}, 1021 cm^{-1}, and 1088 cm^{-1} become significant because of C—O—C band present in chitosan structure and formed by the etherification reaction. FT-IR spectrum of CS-PDMS nanohydrogel shows absorption band at 1010 cm^{-1} for Si—O—Si linkage and at 801 cm^{-1} for Si—CH_3 groups. Different amounts of GDE and PDMS compounds as crosslinkers were added to the emulsion solution of chitosan to prepare crosslinked nanhydrogels. Extraction of the dissolvable portions was carried out in acetic acid aqueous solution to remove uncrosslinked chitosan followed by acetone to remove unreacted PDMS and GDE. It should be noted that chitosan without crosslinker is well soluble in acetic acid aqueous solution. The percent of undissolvable nanohydrogel was calculated after extraction of samples with 1% aqueous acetic acid solution in a refluxing Soxhlet for 12 h. Lower percent of extractable portion implies that there is higher degree of crosslinking. The results in Table 1 show that undissolvable gel percent increases with increasing the initial amount of crosslinker and reaches a maximum value of 90% and 80% when the initial amount of GDE and PDMS were 30 wt% and 20 wt%, respectively. PDMS has long and flexible molecules with many side groups, which form expanded coil conformations inside the networks, and only 20 wt% of PDMS was enough to give maximum gel content.

To observe morphological properties such as surface porosity, texture and roughness, micrographs of the surface and cross-section of the pure chitosan and crosslinked nanohydrogels were registered by using AFM. Fig. 1(a) and (b) shows quite homogeneous surfaces of unmodified chitosan while the crosslinked nanohydrogels of CS-GDE (30%) and CS-PDMS (20%), in Fig. 1(d) and (f), respectively, reveals a predominantly hill-valley-structured surface with irregular pores of nanoscale topography. The roughness on the surface of the crosslinked nanohydrogels can also be seen in 3D images of the surface of samples in Fig. 1(c) and (e), and the size distribution for the nanohydrogel particles of CS-GDE and CS-PDMS are shown in Fig. 1(g) and (h), and the average size are 59.1 nm and 180.3 nm, respectively.

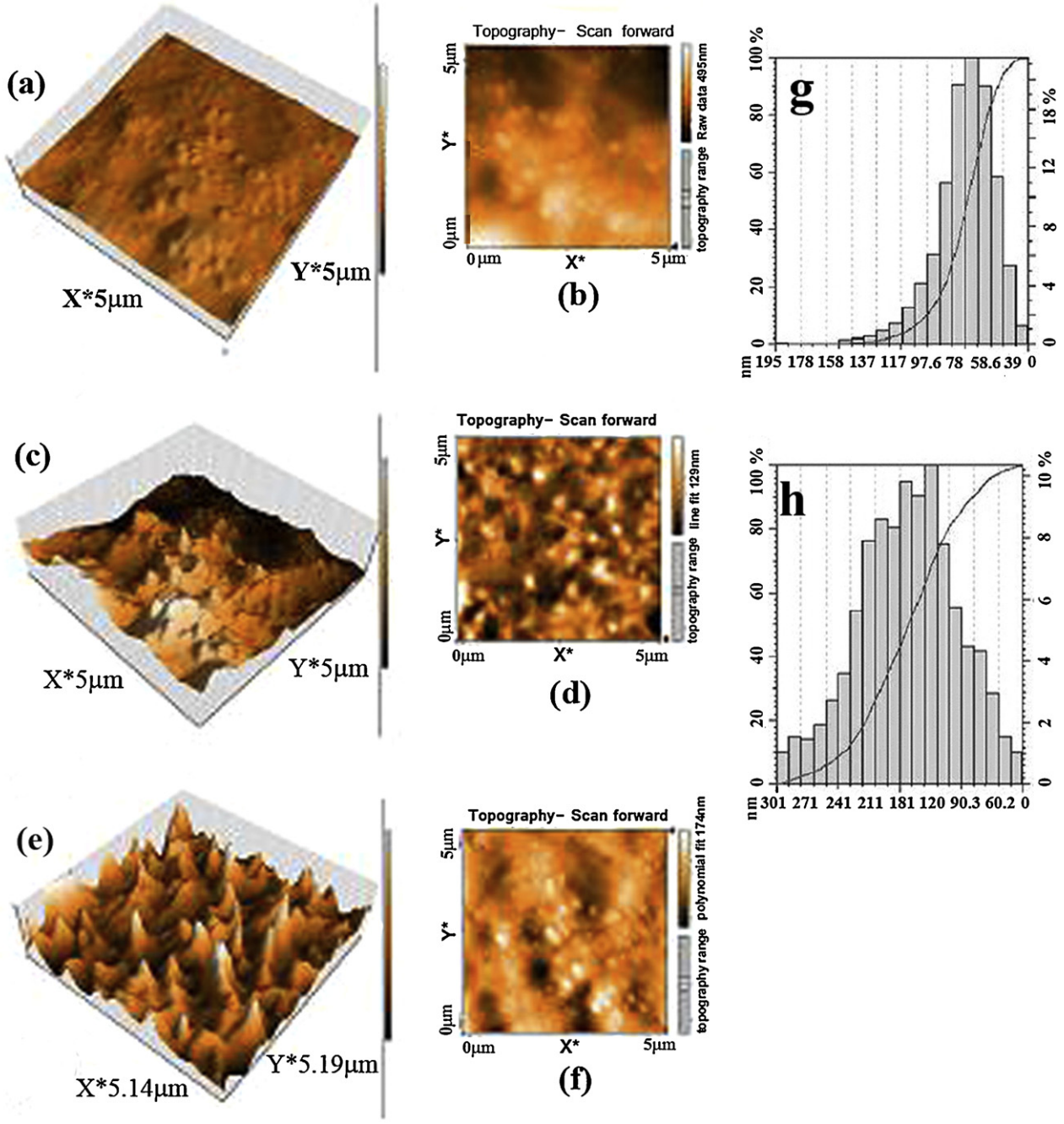

Fig. 1. AFM images of chitosan without crosslinker (a and b), nanohydrogels CS-GDE (30%) (c and d) and CS-PDMS (20%) (e and f), and their histograms (g and h).

3.2. Water swelling behavior of nanohydrogel networks

The linear molecules of chitosan were transformed into the network structure through the crosslinking reactions and water molecules can be preserved in this structure. Fig. 2 shows the water absorption percentage of the crosslinked nanohydrogels CS-GDE and CS-PDMS, respectively, at pH = 7.4 by using sodium phosphate buffer and at room temperature. There is not electrostatic interaction between different functional groups at this pH and the matrices will have opened structures accompanied with maximum water absorption. As can be seen in Fig. 2, increase in the amount of PDMS and GDE resulted in increase in the swellability of nanohydrogels. This can be explained in terms of the nature of bonds inside the matrices structure. It seems that the most important governing forces in swelling are the hydrogen bonding of water molecules with different functional groups present in the nanohydrogels structure such as hydroxyl groups, ether, amine, and unhydrolyzed acetamide linkages. All samples reached equilibrium water content within first 10–20 min of the investigation. The equilibrium water content of nanohydrogels depended on the hydrophilic nature of the crosslinker and the degree of crosslinking. Equilibrium water content of crosslinked nanohydrogels prepared from 30 wt% of GDE and 20 wt% of PDMS was the maximum values of 600% and 450%, respectively. These values were obtained after 30 min immersion in distilled water at room temperature. The water absorption of nanohydrogels prepared from 40 wt% of GDE and 30 wt% of PDMS has decreased indicating that there is a relationship between degree of crosslinking and the amount of

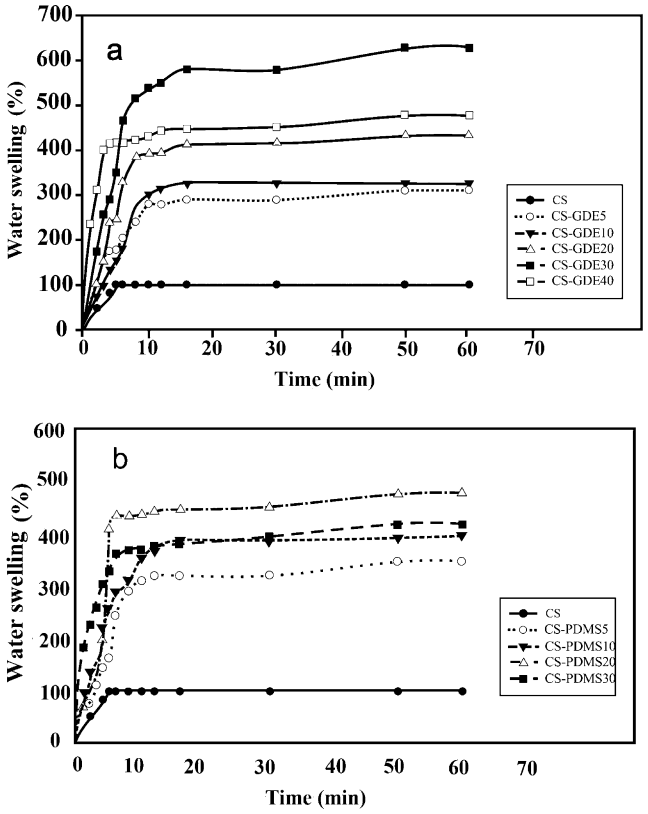

Fig. 2. Swelling behavior of chitosan without crosslinker and nanohydrogels of chitosan with different percents of GDE (a) and PDMS (b) at pH = 7.4 and r.t.

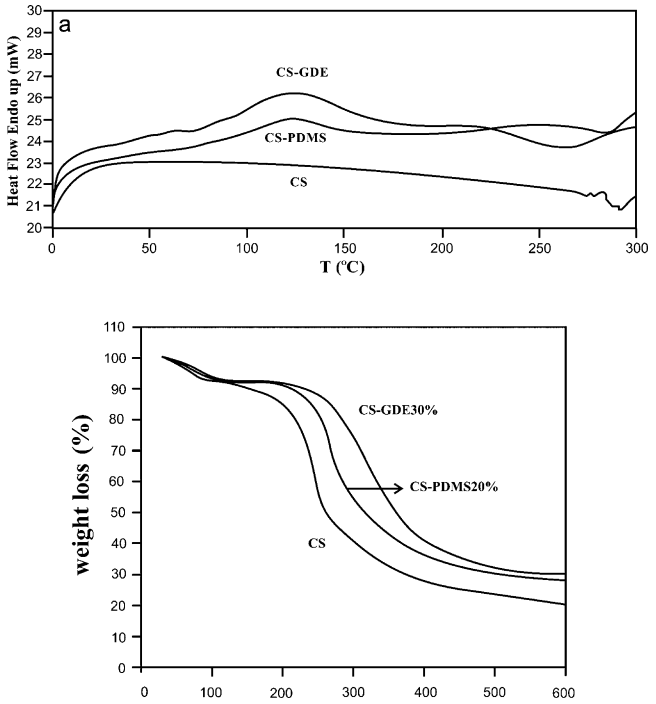

Fig. 3. DSC (a) and TGA (b) curves of chitosan without crosslinker and nanohydrogels of CS-GDE (30%) and CS-PDMS (20%).

water absorption. This can be due to formation of high degree of crosslinks in nanohydrogels. The free volume inside the networks starts to decrease with increase in degree of crosslinking. In general, the water absorption of CS-GDE network was higher than water absorption of CS-PDMS network, as illustrated in Fig. 2(a) and (b). The lower equilibrium water content of CS-PDMS network can be due to presence of large aggregate of hydrophobic coils of PDMS molecules inside the network. However, the significant increase of equilibrium water content in a short period of time was probably due to the presence of microphase separation of PDMS amphiphile in chitosan matrix which resulted in significant increase of surface area of chitosan owing to porous-like morphology.

The results indicate that water absorption of nanohydrogel samples depend on the pH value. The water absorption is maximum at pH = 7–8 and decrease at high and low pH values. This can be due to structural changes in the network under acidic and basic conditions. The water absorption percent increase with increasing temperature, which is due to expansion of the crosslinked network to some extent. However, the absorbed water at room temperature remains constant with time while at higher temperatures (40 °C and 60 °C) reaches to a maximum and then starts to decrease with increasing time period. The higher is the temperature the faster is the loss of absorbed water. This is due to the instability of hydrogen bonds between functional groups of the network and water molecules at higher temperatures.

3.3. Thermal properties of nanohydrogel networks

Fig. 3a shows DSC curves of CS-GDE (30%) and CS-PDMS (20%) nanohydrogels under N_2 atmosphere at the heating rate of 10 °C/min. As can be seen in this figure, there is an endothermic peak in the temperature range of 100–150 °C indicating the loss of water molecules which are trapped inside the networks and have not been removed during initial drying in the oven. There are also small exothermic peaks in the DSC curves of nanohydrogels above 250 °C. These peaks can be related to the crosslinking reaction between unreacted epoxide groups with the hydroxyl groups (etherification reaction usually occurs at >200 °C) or thermal decomposition.

The thermal stability of neat chitosan, CS-GDE (30%) and CS-PDMS (20%) nanohydrogels was evaluated by TGA under N_2 atmosphere at heating rate of 10 °C/min. As can be seen in Fig. 3b, TGA curves consist of three parts; the first part up to 100 °C of 10 wt% loss for CS-PDMS sample and to 180 °C of 20 wt% loss for CS-GDE sample is related to dehydration. The pure chitosan and CS-PDMS nanohydrogels have less moisture and dehydrated faster than CS-GDE nanophydrogels. The second part is a thermal degradation stage resulting from pyrolysis which starts from about 200 °C and ended at 400 °C with loss of 66 wt% and 50 wt% for CS-PDMS and CS-GDE, respectively. The third part represents the conversion of the remaining materials to carbon residues. The residual weights are 30 wt% and 18 wt% at 600 °C for modified and neat chitosan, respectively.

3.4. Drug loading and releasing efficiency of nanohydrogel networks

Nanohydrogel networks with the highest water swellability, CS-GDE (30%) and CS-PDMS (20%), were used for SDF loading at pH = 7.4 and room temperature. The amount of loaded SDF was determined by using the calibration curve which was made by reading absorption of SDF at 276 nm for different amounts of SDF in distilled water. The percent of loaded SDF increased with increasing the initial amount of SDF and reached a maximum of 80% for CS-GDE and 60% for CS-PDMS nanohydrogels when the initial amount of SDF was 0.75%, as shown in Fig. 4a. SDF loading decreased when the initial amount of SDF was 1%, which can be due to the fact that 1% SDF did not dissolve completely in water at pH = 7.4 and room temperature. As can be seen in Fig. 4a, the loading efficiency of CS-GDE is higher than the loading efficiency of CS-PDMS. The higher the swellability

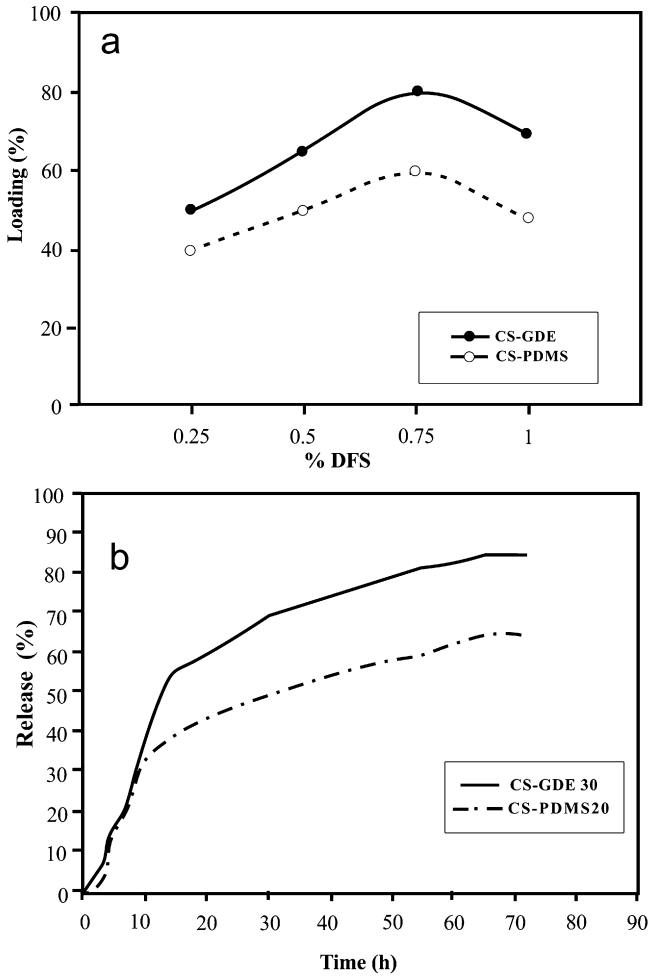

Fig. 4. DFS loading (a) and release (b) curves of nanohydrogels of CS-GDE (30%) and CS-PDMS (20%).

of nanohydrogel the higher the loading of SDF will be. This can be related to the hydrophobic nature of PDMS and also due to PDMS chain aggregates inside the networks.

Fig. 5 shows SEM images of unloaded and loaded nanohydrogels of CS-GDE (30%). It can be seen that there is smooth structure and no pores or cracks on the surface for the unloaded nanohydrogels, Fig. 5(a), in comparison with the rough surface with cracks for the loaded sample, as shown in Fig. 5(b). This confirms the miscibility of the prepared nanohydrogels with the SDF.

To determine the potential application of chitosan nanohydrogels containing a pharmaceutically active compound, we have investigated drug release behavior from these systems. The SDF release efficiency was studied in buffered solution at pH = 7.4 and 37 °C for samples with the maximum loading (initial amount of 0.75%). The choice of buffered solution was due to the maximum swelling of nanohydrogels at this pH. At specific time intervals, 3 mL solution was withdrawn from inside of the releasing flask and concentration of the released SDF was determined by reading the absorption of the filtrate at 276 nm and using the calibration curve. As can be seen in Fig. 4(b), the cumulative release ratio of SDF from the nanohydrogels of CS-GDE (30%) and CS-PDMS (20%) increased with time and reached to the maximum of 85% and 62%, respectively, at the end of experiment (after 70 h). The higher the swellability of nanohydrogel the higher the release of SDF will be. Logically, the diffusion of the drug is easier in more opened–swelled structure than that in more compact structure.

Table 2
Separation of BSA protein from pure CS hydrogel network.

Protein yield (%)	Total protein (mg)	Buffer volume (mL)	No.
–	20.00	1.0	Initial
15.3	3.06	12.0	1
14.1	2.82	12.0	2
13.3	2.66	12.0	3
10.1	2.02	8.0	4
52.8	10.56	44	Total

3.5. Embedding of magnetic Fe_3O_4 nanoparticles into hydrogel network

Chemical precipitation such as co-precipitation of ferric (Fe^{3+}) and ferrous (Fe^{2+}) ions is comparatively the simplest, and is commonly used for the preparation of Fe_3O_4, and provides relatively a good control over the size and morphology of the nanoparticles (Peng et al., 2004). The X-ray pattern of magnetic Fe_3O_4 nanoparticles showed characteristic peaks at $2\theta = 21.0°$, 35.4°, 43.5°, 53.4°, 61.2°, 68.4° and 73.0° which are consistent with those reported by Huang, Liao, and Chen (2003). The particles exhibited strong magnetic response and had mean diameter of 12.8 nm which was measured according to the method given in the literature by using Debye–Scherrer equation (Yu et al., 2009).

Embedded magnetic Fe_3O_4 nanoparticles–hydrogel composite was prepared via the alkali hydrolysis of a mixture of iron oxides in the matrix of a chemically crosslinked hydrogel of chitosan with GDE. The insertion of magnetic nanoparticles into the chitosan-based hydrogel network was examined by taking AFM images which are shown in Fig. 5(c) and (d). One can see some dotted area in Fig. 5(c) indicating that nanoparticles were almost uniformly distributed and strongly adhered on the network. As can be seen in Fig. 5(d), the paramagnetic Fe_3O_4 nanoparticles on the network are unidirectional directed in a magnetic field.

3.6. Separation of BSA protein from neat hydrogel and magnetite-hydrogel networks

To quantify the protein separation using chitosan hydrogels, the following relationships were used (Nelson & Cox, 2008). Protein yield was defined as mass of BSA at a given step divided by total mass of BSA in the crude extract. In these experiments, the crude extract that was actually the initial feed of the column, contained 20 mg BSA.

$$\text{protein yield} = \frac{\text{mass of BSA at each step}}{\text{total mass of BSA in the crude extract}}$$

For comparison, BSA protein, under the optimized elution conditions, was purified by passing the solution through a column filled of neat chitosan hydrogel network. The data are shown in Table 2. The purified samples were defined such that the initial sample was introduced to the column and purified to make sample 1. Then sample 1 was recycled to the column and further purified to make sample 2. Accordingly, samples 3 and so were defined. Total protein decreases because the objective is to remove unwanted or nonspecific protein as much as possible. Table 2 indicates that after 4 steps of purification, 52.8% of the total protein in the bulk solution was adsorbed and separated by the neat chitosan hydrogel.

The immobilization of BSA protein on the Fe_3O_4 nanoparticles was carried out in the presence of carbodiimide during formation of cross-linked hydrogel network of CS-GDE. As a catalyst, carbodiimide is used to activate a carboxyl group in BSA molecule and to bind protein directly on magnetic particles (Peng et al., 2004). BSA is an amphiphilic protein due to the presence of a NH_2 and a COOH group in its molecular structure. It shows a different net charge at different pH media. The isoelectric point of bovine serum albumin

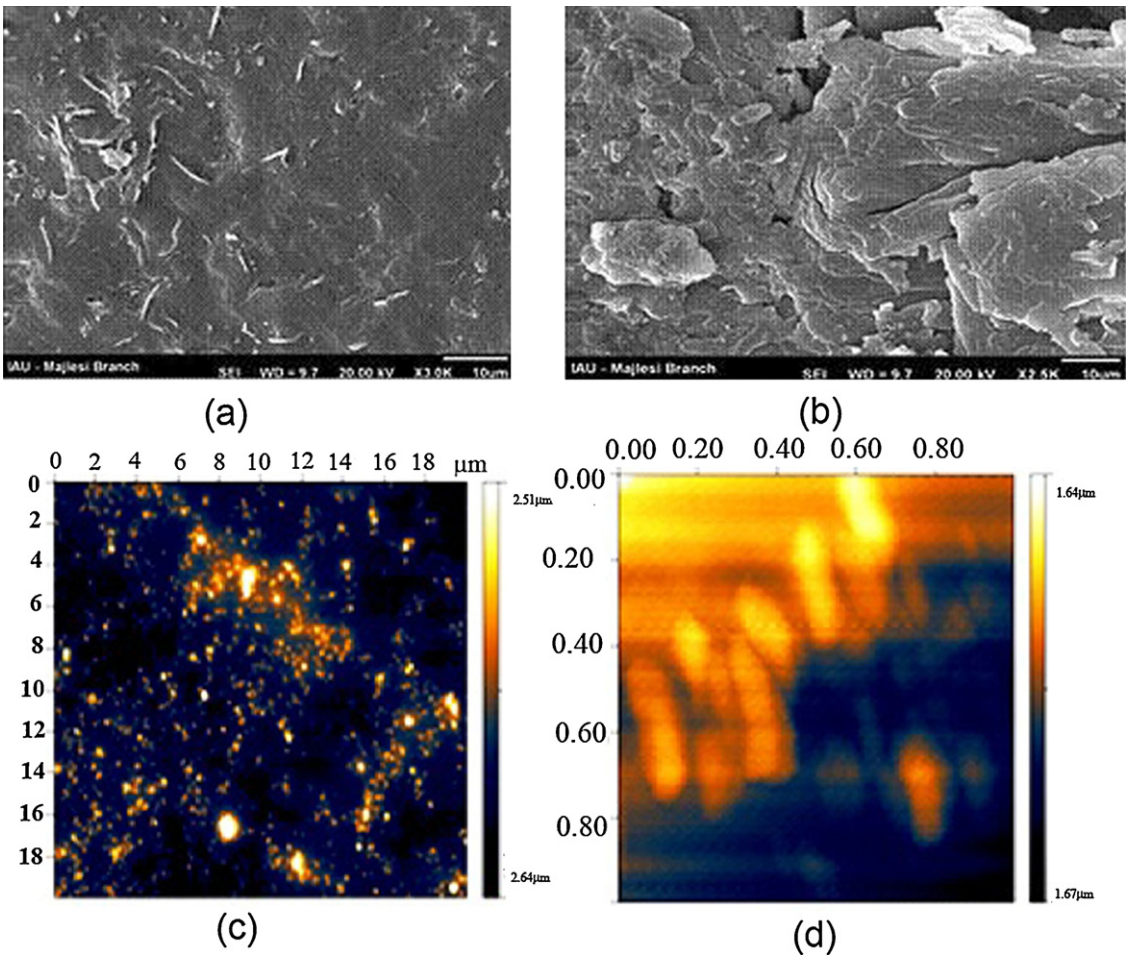

Fig. 5. SEM images of unloaded (a) and DFS loaded (b) nanohydrogels of CS-GDE (30%) AFM images (c and d) of Fe_3O_4 nanoparticles in the chitosan hydrogel network.

Table 3
Separation of BSA protein from magnetic-CS hydrogel network.

Protein yield (%)	Total protein (mg)	D_{90} (μm)	D_{50} (μm)	D_{10} (μm)	D_{av} (μm)	Magnetic adsorbent
–	20	88	44	16	48	Initial sample
36.25	7.25	126	60	24	64	1st stage separation
44.25	8.85	142	64	28	72	2nd stage separation
80.5	16.1	–	–	–	–	Total

is pH = 4.7. It indicates that BSA has a positive charge below pH 4.7 and negative charge above pH 4.7. The covalently bounded BSA protein on the Fe_3O_4 nanoparticles which has been embedded into the chitosan hydrogel networks was used to separate BSA protein from a bulk solution in an electromagnetic separator. Table 3 shows the size distribution of the magnetic affinity adsorbents before and after the magnetic separator treatment. D_{av} represents the average diameter of the particles. D_{10}, D_{50} and D_{90} parameters indicate that 10%, 50% and 90% of particles have smaller diameter than the value given in the table. Size distribution of the magnetic particles was determined using the particle size analyzer Cilas 920 L (France). As a result, at the end of the experiments, 80.5% of BSA was separated from the initial chitosan hydrogel solution in the magnetic separator. Each sample data in Table 3 represent the results corresponding to the each step of the separation. Comparing the data given in Tables 2 and 3 reveal that chitosan hydrogel network with immobilized Fe_3O_4 nanoparticles considerably increased the BSA purification yield and decreased the required time to reach to the certain level of purification compared to the neat chitosan hydrogel network. The purification yield increased from 52.8% after 4 steps of purification to about 80.5% after 2 steps of purification. The present study suggests that Fe_3O_4 magnetic nanoparticles can be used in separation of BSA proteins from polysaccharide solutions.

4. Conclusion

Crosslinked nanohydrogels of chitosan with different percents of GDE and PDMS were effectively prepared in an emulsion media. High percent of crosslinked nanogels (92%) with average size of 59 nm were obtained from chitosan and low molecular weight GDE in comparison with 80% nanogels with average size of 180 nm obtained with hydrophobic high molecular weight PDMS. The equilibrium water content of the nanohydrogels showed dependence on the temperature, pH, degree of crosslinking, and chemical structure of crosslinker. The nanohydrogels obtained from chitosan and 30 wt% GDE reached equilibrium water content of 600% for 20 min at pH 7.4 and room temperature. Thermal decomposition temperature of 250 °C for nanogels as compared to neat chitosan (160 °C) was evidenced by TGA analysis. The crosslinked nanohydrogels

were used as carriers for SDF and 80% release was obtained at pH 7.4 and 37 °C. The other object of this study was to optimize the chitosan hydrogel network for using it in protein purification. First, the ability of neat chitosan hydrogel network to separation and purification of BSA was examined, and it was obtained around 52.8% under optimized separation conditions. Then, immobilized BSA protein on the super paramagnetic Fe_3O_4 nanoparticles (9.8 nm) into the chitosan hydrogel network was prepared in a simultaneous process. Finally, protein and magnetic nanoparticles were separated from volumes of suspension solution in one magnetic separator using a magnetic field with a yield of separation of 80.5%. The advantages of magnetic separation are attributed to its speed, accuracy, and simplicity.

Acknowledgements

Financial support of this Project by the University of Mazandaran (Iran) is gratefully acknowledged. Authors acknowledge Mr. M. Sadeghi Sarokolaei (Department of Biotechnology, University of Isfahan, Esfahan, Iran) for his assistance in the magnetite-separation of BSA and analysis.

References

Ah, L., Salabas, E., & Schuth, F. (2007). Magnetic nanoparticles: Synthesis, protection, functionalization, and application. *Angewandte Chemie International Edition*, *46*(8), 1222–1244.

Bajpai, S. K., & Rasika, T. (2006). Investigation of water uptake behavior and stability of calcium alginate/chitosan bi-polymeric beads: Part-1. *Reactive and Functional Polymers*, *66*, 645–658.

Bernkop-Schnurch, A., & Walker, G. (2001). Multifunctional matrices for oral peptide delivery. *Critical Reviews in Therapeutic Drug Carrier Systems*, *18*(5), 459–501.

Borzacchiello, A., Ambrosio, L., Netti, P., Nicolais, L., Peniche, C., Gallardo, A., et al. (2001). Chitosan-based hydrogels: Synthesis and characterization. *Journal of Material Sciences: Materials in Medicine*, *12*, 861–864.

Chen, G., & Hoffman, A. S. (1995). Graft copolymers that exhibit temperature induced phase transitions over a wide range of pH. *Nature*, *373*, 49–52.

Enescu, D., Hamciucb, V., Ardeleanub, R., Cristeab, M., Ioanidb, A., Harabagiub, V., et al. (2009). Polydimethylsiloxane modified chitosan. Part III: Preparation and characterization of hybrid membranes. *Carbohydrate Polymers*, *76*, 268–278.

Fan, Y. F., Wang, Y. N., Fan, Y. G., & Ma, J. B. (2006). Preparation of insulin nanoparticles and their encapsulation with biodegradable polyelectrolytes via the layer-by-layer adsorption. *International Journal of Pharmaceutics*, *324*(2), 158–167.

Felt, O., Buri, P., & Gurny, R. (1998). Chitosan: A unique polysaccharide for drug delivery. *Drug Delivery and Industrial Pharmaceuticals*, *24*, 979–993.

George, M., & Abraham, T. E. (2006). Polyionic hydrocolloids for the intestinal delivery of protein drugs: Alginate and chitosan—A review. *Journal of Controlled Release*, *114*(1), 1–14.

Hirano, S., Yamaguchi, Y., & Kamiya, M. (2003). Water-soluble N-(n-fatty acyl) chitosans. *Macromolecular Bioscience*, *3*, 629–631.

Huang, S. H., Liao, M. H., & Chen, D. H. (2003). Direct binding and characterization of lipase onto magnetic nanoparticles. *Biotechnology Progress*, *19*, 1095–1100.

Kato, Y., Onishi, H., & Machida, Y. (2003). Application of chitin and chitosan derivatives in the pharmaceutical field. *Current Pharmaceutical Biotechnology*, *4*(5), 303–309.

Kumar, M. N. V. R., Muzzarelli, R. A. A., Muzzarelli, C., Sashiwa, H., & Domb, A. J. (2004). Chitosan chemistry and pharmaceutical perspectives. *Chemical Reviews*, *104*, 6017–6084.

Mehta, R. V., Upadhyay, R. V., Charles, S. W., & Ramchand, C. N. (1997). *Biotechnology Techniques*, *11*, 493–496.

Muzzarelli, R. A. A. (2009). Chitins and chitosans for the repair of wounded skin, nerve, cartilage and bone. *Carbohydrate Polymers*, *76*, 167–182.

Muzzarelli, R. A. A. (2011). Chitosan composites with inorganics, morphogenetic proteins and stem cells, for bone regeneration. *Carbohydrate Polymers*, *83*, 1433–1445.

Muzzarelli, R. A. A. (2010). Chitins and chitosans as immunoadjuvants and non-allergenic drug carriers. *Marine Drugs*, *8*(2), 292–312.

Muzzarelli, R. A. A., Boudrant, J., Meyer, D., Manno, N., DeMarchis, M., & Paoletti, M. G. (2012). Current views on fungal chitin/chitosan, human chitinases, food preservation, glucans, pectins and inulin: A tribute to Henri Braconnot, precursor of the carbohydrate polymers science, on the chitin bicentennial. *Carbohydrate Polymers*, *87*, 995–1012.

Muzzarelli, R. A. A., Greco, F., Busilacchi, A., Sollazzo, V., & Gigante, A. (2012). Chitosan, hyaluronan and chondroitin sulfate in tissue engineering for cartilage regeneration: A review. *Carbohydrate Polymers*, *89*, 723–739.

Nelson, D., & Cox, M. M. (2008). (fourth ed.). *Lehninger principles of biochemistry* University of Wisconsin-Madison., pp. 96–97. ISBN: 0-7167-5752-7.

Pandey, R., Ahmad, Z., Sharma, S., & Khuller, G. K. (2005). Nano-encapsulation of azole antifungals: Potential applications to improve moral. *International Journal of Pharmaceutics*, *301*(1–2), 268–276.

Peng, Z. G., Hidajat, K., & Uddin, M. S. (2004). Adsorption of bovine serum albumin on nanosized magnetic particles. *Journal of Colloid and Interface Science*, *271*, 277–283.

Prabaharan, M., & Mano, J. F. (2006). Stimuli-responsive hydrogels based on polysaccharides incorporated with. *Macromolecule Bioscience*, *6*(12), 991–1008.

Sashiwa, H., Yamamori, N., Ichinose, Y., Sunamoto, J., & Aiba, S. (2003). Chemical modification of chitosan. 17a. Michael reaction of chitosan with acrylic acid in water. *Macromolecular Bioscience*, *3*, 231–233.

Senel, S., & McClure, S. J. (2004). Potential applications of chitosan in veterinary medicine. *Advanced Drug Delivery Reviews*, *56*, 1467–1480.

Sharma, S., Kulkarni, J., & Pawar, A. P. (2006). Permeation enhancers in the transmucosal delivery of macromolecules. *Die Pharmazie*, *61*(6), 495–504.

Shutava, T. G., & Lvov, Y. M. (2006). Nano-engineered microcapsules of tannic acid and chitosan for protein? *Journal of Nanoscience and Nanotechnology*, *6*(6), 1655–1661.

Sokker, H. H., Abdel Ghaffar, A. M., Gad, Y. H., & Aly, A. S. (2009). Synthesis and characterization of hydrogels based on grafted chitosan for the controlled drug release. *Carbohydrate Polymers*, *75*, 222–229.

Tao, S., Pang, R., Chen, C., Ren, X., & Hu, S. (2012). Synthesis, characterization and slow release properties of O-naphthylacetyl chitosan. *Carbohydrate Polymers*, *88*, 1189–1194.

van der Lubben, I., Verhoef, J. C., Borchard, G., & Junginger, H. E. (2001). Chitosan for mucosal vaccination. *Advanced Drug Delivery Reviews*, *52*(2), 139–144.

Verma, A. J., Deshpande, S. V., & Kennedy, J. K. (2004). Graft copolymerization of vinyl monomers onto chitosan. *Carbohydrate Polymers*, *55*, 77–93.

Wang, T.-H., & Lee, W.-C. (2003). Immobilization of proteins on magnetic nanoparticles. *Biotechnology and Bioprocess Engineering*, *8*, 263–267.

Yanga, C., Ling, X., Zhou, Y., Zhang, X., Huang, X., Wang, M., et al. (2010). A green fabrication approach of gelatin/CM-chitosan hybrid hydrogel for wound healing. *Carbohydrate Polymers*, *82*, 1297–1305.

Yu, C. H., Al-Saadi, A., Shih, S.-J., Qiu, L., Tam, K. Y., & Tsang, S. C. (2009). Immobilization of BSA on silica-coated magnetic iron oxide nanoparticle. *Journal of Physical Chemistry C*, *113*, 537–543.

Yu, S., Hu, J., Pan, X., Yao, P., & Jiang, M. (2006). Stable and pH-sensitive nanogels prepared by selfassembly of chitosan and ovalbumin. *Langmuir*, *22*, 2754–2759.

Zhou, Y., Yang, Y., Wang, D., & Liu, X. (2003). Preparation and characterization of 6-carboxychitosan. *Chemistry Letters*, *32*, 682–683.